VOLUME 10 | ISSUE3

Head and Neck Imaging

ORIGINAL ARTICLE

Morphological Characterization of the Pterygoid Hamulus Using Cone Beam Computed Tomography

Dr. Karthikeya Patil-MDS, Dr. Sanjay C J-MDS, Dr. Monica Mirnalini M N, Dr. Varusha Sharon Christopher-BDS, Dr. Eswari Solayappan-BDS

Department of Oral Medicine and Radiology, JSS Dental College and Hospital, JSS Academy of Higher Education and Research, Mysuru - 570015 Karnataka, India

SUBMISSION: 26-8-2024 | ACCEPTANCE: 26-5-2025

ABSTRACT

Purpose: To evaluate the morphological characteristics of the pterygoid hamulus (PH) using cone beam computed tomography (CBCT), assessing its length, width, interpterygoid distance, and spatial relationships with the posterior nasal spine (PNS) across different age groups and genders.

Materials and Methods: This retrospective study analysed CBCT images of 100 subjects (50 males, 50 females) from various age groups. Measurements included PH length and width bilaterally, interpterygoid distance, distance from PH to PNS, and the angle formed between PH and PNS. Statistical analyses were performed to assess differences between sides, genders, and age groups.

Results: Significant bilateral asymmetry was observed in PH length ($p<0.001$) and width ($p=0.003$), with the right side generally being shorter but wider. Males exhibited greater PH width compared to females ($p = 0.002$ for the right side). PH length showed age-related variations, increasing from under 20 years to 21-59 years, then slightly decreasing in those over 60. The angle between PH and PNS was significantly larger on the left side ($p<0.001$). Interpterygoid distance remained relatively consistent across age groups and genders.

Conclusion: This study provides comprehensive morphometric data on the pterygoid hamulus, revealing significant bilateral asymmetries and gender-related differences. These findings contribute to the

CORRESPONDING AUTHOR, GUARANTOR

Dr. Sanjay CJ, MDS, Reader. Department of Oral Medicine and Radiology, JSS Dental College and Hospital , JSS Academy of Higher Education and Research Mysuru - 570015 Karnataka, India
E mail: drsanjaycj_dch@jssuni.edu.in
Contact Number: +91 97425 65566

understanding of PH anatomical variations and have important implications for various dental and maxillofacial procedures, potentially enhancing diagnostic accuracy, treatment planning, and surgical outcomes.

KEY WORDS Pterygoid hamulus, posterior nasal spine, bursitis, Cone beam computed tomography, orofacial pain

Introduction

The pterygoid hamulus, a hook-like bony projection of the medial pterygoid plate of the sphenoid bone, is a small yet significant anatomical structure in the craniofacial region. Located on the posterior aspect of the hard palate, this structure serves as an important landmark and attachment point for various soft tissue components. The hamulus plays a crucial role in the biomechanics of the oral and pharyngeal regions by providing a pulley for the tensor veli palatini muscle and serving as an attachment site for the pterygomandibular raphe [1].

Despite its small size, the pterygoid hamulus has garnered increasing attention in clinical practice due to its potential involvement in various orofacial pain syndromes, including hamular bursitis, elongated hamulus syndrome, and dysphagia. Moreover, its proximity to critical neurovascular structures and its relevance in surgical procedures, such as cleft palate repair and pterygomaxillary disjunction, underscore the importance of a thorough understanding of its morphology and anatomical relationships [2].

Dry skull studies, while historically valuable, have inherent limitations that can compromise their applicability in modern clinical practice [2–4]. These studies often rely on a limited number of specimens, which may not adequately represent the diverse morphological variations present across different populations, ages, and sexes. Furthermore, the process of skull preparation can potentially alter delicate anatomical structures, leading to measurement inaccuracies. The static nature of dry skulls also fails to account for the dynamic relationships between hard and soft tissues in living individuals. In contrast, cone beam computed tomography (CBCT) studies offer a more comprehensive and accurate approach to craniofacial analysis [5].

CBCT allows for non-invasive, in vivo examination of anatomical structures in three dimensions, preserving spatial relationships and soft tissue context. This imaging modality enables researchers to conduct large-scale studies across diverse populations, capturing a wide range of anatomical variations and providing more representative data. The ability to perform retrospective analyses on CBCT datasets further enhances the statistical power and clinical relevance of these studies. Hence, the aim of this study is to evaluate the morphological characteristics of the pterygoid hamulus using cone beam computed tomography, assessing its length, width, and spatial relationships with the surrounding structures across different age groups and genders, to provide comprehensive morphometric data that can be clinically applied in dentistry and maxillofacial therapeutics for individualised treatments.

Materials and Methods

A descriptive retrospective study was conducted on 100 CBCT images that were sourced from the archived data of subjects who were scrutinised for developmental anomalies, trauma, implant planning, and pre-surgical planning of orthognathic surgery, who reported to the department from March 2023 to March 2024. Ethical clearance was obtained from the institutional ethics committee for monocentric setting. The volumetric images produced in the large view modes were generated using Planmeca ProMax 3D Mid. Samples were selected using a convenient sampling method, assuming an absolute precision of 5% and a confidence level of 95%.

Inclusion criteria:

- Ideal coronal section of optimum diagnostic CBCT images of pterygoid hamulus and closely associated structures.
- Patients who underwent full face or midface CBCT evaluation for:

- mixed dentition analysis,
- maxillary and mandibular arch pathologies,
- Pre and post treatment evaluation for maxillofacial implant placement and orthodontic treatment
- pre-surgical planning for orthognathic surgery, and
- trauma involving the maxilla as well as the mandible.

Exclusion criteria:

- CBCT of coronal images does not clearly depict the base of the skull, especially the pterygoid hamulus.
- Images with radiological evidence of developmental defects or pathology involving the base of the skull.
- Inadequate image quality includes images with exposure artefacts, subject artefacts, and inherent artefacts.

Radiographic images satisfying this inclusion criteria were analysed for coronal, sagittal, and 3D-rendered images in Planmeca Romexis 5.3 (3D software), The following were the parameters analysed;

- Length of the pterygoid hamulus on the right and left side (Figure 1A)
- Width of the pterygoid hamulus on the right and left side (Figure 1B)
- Inter - pterygoid distance (Figure 1C)
- Distance from pterygoid hamulus to posterior nasal spine (PNS) on right and left side (Figure 1D).
- Angle formed between the pterygoid hamulus and the posterior nasal spine (PNS) on the right (Figure 1E) and left side (Figure 1F).

Statistical Analysis:

Statistical analysis was carried out using SPSS version 22 for both qualitative and quantitative data. Independent t tests and paired t tests were carried out to find sexual morphometrics and any bilateral variance, respectively. An ANOVA test was used to compare the parameters among different age groups. The demographic data was evaluated using descriptive statistics. A p value less than 0.05 will be considered statistically significant.

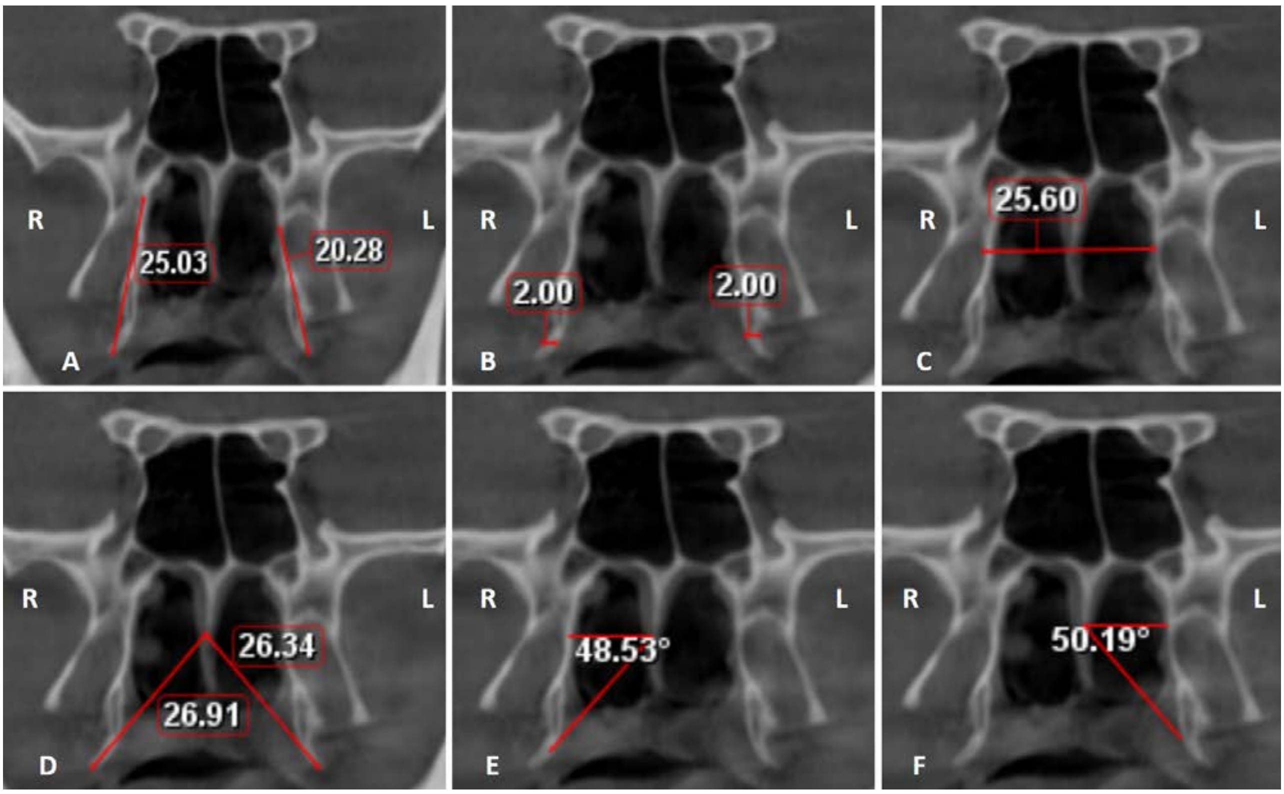

Figure 1A: *Coronal view shows length of PH;*
Figure 1B: *shows width of the PH;*
Figure 1C: *Shows distance between right and left pterygoid process;*
Figure 1D: *Shows distance from pterygoid hamulus to posterior nasal spine;*
Figure 1E and 1F: *Shows angle formed between the pterygoid hamulus and the posterior nasal spine*

Results

Descriptive statistics revealed significant disparities between the genders. The right PH has an average length of 20.646 mm in females and 21.982 mm in males, while the left PH has an average length of 22.698 mm in females and 23.533 mm in males. In females, the right PH width is an average of 1.763 mm, while in males it is 2.504 mm. The left PH width is 1.746 mm in females and 2.063 mm in males. The lengths and angles from the PNS to the PH and inter-pterygoid distance, among other measurements, exhibit minor variations between sexes but generally lie within relatively limited ranges. (Table 1)

Descriptive statistics for the pterygoid hamulus across age categories shows that right PH length increases from 19.481 mm in individuals under 20 to approximately 22 mm in the 21-59 age group, and then slightly decreases to 21.662 mm in those over 60.

The left PH length is lowest in the under 20 group at 21.073 mm and reaches its maximum at 23.874 mm in those over 60. The under-20 group exhibits the greatest right PH width at 2.234 mm. The PNS to PH length exhibits minor variations, with the 41-59 age group exhibiting the highest measurements.

The right angle of PNS to PH increases with age, from 47.272 degrees in individuals under 20 to 49.553 degrees

Table 1: Descriptive statistics between gender and parameters

Parameters	Sex	Mean	Std. Deviation	Minimum	Maximum
Right: length of PH (in mm)	Female	20.646	3.931	13.690	25.910
	Male	21.982	3.346	15.780	25.910
Left - Length of PH (in mm)	Female	22.698	3.568	16.100	28.040
	Male	23.533	3.820	15.380	28.040
Right - Width of PH (in mm)	Female	1.763	0.824	0.000	3.200
	Male	2.504	1.449	0.000	4.800
Left - Width of PH (in mm)	Female	1.746	0.687	0.800	2.800
	Male	2.063	1.072	0.600	4.200
Right Length of PNS to PH (in mm)	Female	26.637	3.308	21.200	35.190
	Male	26.875	3.074	23.790	35.190
Left Length of PNS to PH (in mm)	Female	25.757	3.543	18.750	35.080
	Male	26.472	2.812	22.210	35.080
Right Angle of PNS to PH (in °)	Female	48.147	4.175	40.840	58.010
	Male	48.917	3.531	43.240	58.010
Left Angle of PNS to PH (in °)	Female	50.689	6.033	35.650	56.640
	Male	51.598	3.425	44.560	56.260
Inter-pterygoid Distance (in mm)	Female	28.426	2.405	25.600	32.400
	Male	28.626	2.028	26.000	32.400

Table 2: Descriptive statistics between age group and parameters

Parameters	Age Group	Mean	Std. Deviation	Minimum	Maximum
Right - Length of PH (in mm)	<20	19.481	3.876	13.690	24.730
	21-40	22.027	2.875	16.380	25.910
	41-59	22.086	4.318	13.690	25.910
	>60	21.662	3.092	15.780	25.620

Table 2: Descriptive statistics between age group and parameters

Parameters	Age Group	Mean	Std. Deviation	Minimum	Maximum
Left - Length of PH (in mm)	<20	21.073	3.948	15.380	28.040
	21-40	23.880	3.227	15.380	28.040
	41-59	23.637	3.654	16.100	28.040
	>60	23.874	3.365	15.380	28.040
Right - Width of PH (in mm)	<20	2.234	1.268	0.000	4.800
	21-40	1.980	1.436	0.000	4.800
	41-59	2.108	0.912	0.500	4.020
	>60	2.213	1.305	0.000	4.800
Left - Width of PH (in mm)	<20	2.056	1.041	0.800	4.200
	21-40	1.865	1.048	0.600	4.200
	41-59	1.846	0.690	0.900	2.800
	>60	1.852	0.852	0.600	4.200
Right - Length of PNS to PH (in mm)	<20	26.517	3.389	21.200	35.190
	21-40	26.448	2.579	23.790	35.190
	41-59	27.203	3.855	21.200	35.190
	>60	26.855	2.883	23.790	35.190
Left - Length of PNS to PH (in mm)	<20	24.821	3.420	18.750	35.080
	21-40	26.463	2.308	22.210	35.080
	41-59	26.680	4.160	18.750	35.080
	>60	26.495	2.371	22.210	35.080
Right - Angle of PNS to PH (in ˚)	<20	47.272	4.243	40.840	58.010
	21-40	47.921	3.062	43.240	58.010
	41-59	49.382	4.503	40.840	58.010
	>60	49.553	3.181	43.240	58.010
Left - Angle of PNS to PH (in ˚)	<20	49.442	6.319	35.650	56.640
	21-40	52.371	3.293	44.560	56.640
	41-59	51.140	5.960	35.650	54.130
	>60	51.620	2.829	44.560	56.260
Inter-pterygoid Distance (in mm)	<20	28.756	2.431	25.600	32.400
	21-40	28.058	1.995	25.600	31.000
	41-59	28.577	2.123	26.000	31.600
	>60	28.714	2.352	26.000	32.400

in those over 60. Across age categories, the inter-pterygoid distance remains consistent, ranging from 28.058 mm to 28.756 mm. (Table 2)

A paired sample t-test was employed to compare the measurements of the pterygoid hamulus on the right and left sides. The results showed a substantial difference in the length of the PH between the right and left sides ($t = -6.802$, $df = 99$, $p < .001$), with the right side being shorter. The right side of the PH was substantially wider ($t = 3.051$, $df = 99$, $p = 0.003$).

In addition, the length of the PNS to the PH varied significantly between the two sides ($t = 2.811$, $df = 99$, $p = 0.006$), with the right side being longer. Similarly, the angle between the PNS and PH was substantially different ($t = -6.204$, $df = 99$, $p < .001$), with the right side exhibiting a shortened angle. (Table 3 and Figure 2)

An independent sample t-test showed that males had wider PH measurements than females, with a significant difference in the width of the PH on the right (t = -3.143, df = 98, p = 0.002) and left sides (t = -1.759, df = 98, p = 0.082). Conversely, no substantial disparities were identified in the length of the PH or the distance from the PNS to the PH between the sexes. Similarly, the angles of PNS to PH and inter-pterygoid distance did not exhibit significant differences between males and females. The results of these studies indicate that the pterygoid hamulus width varies between sexes, but other parameters are comparable. (Table 4 and Figure 3)

Table 3: Paired sample t test

Doppler Indices	t	df	p
Right - Left : Length of PH (in mm)	-6.802	99	***< .001***
Right - Left : Width of PH (in mm)	3.051	99	***0.003***
Right - Left : Length of PNS to PH (in mm)	2.811	99	***0.006***
Right - Left: Angle of PNS to PH (in ˚)	-6.204	99	***< .001***

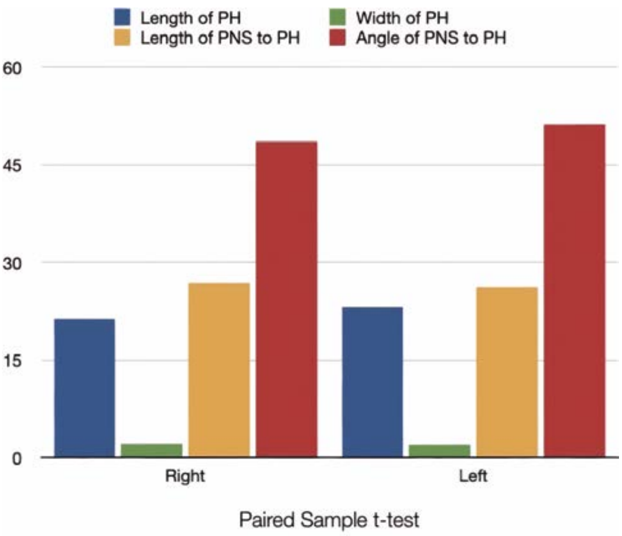

Figure 2: *Paired Sample t - test for bilateral variance in pterygoid hamulus*

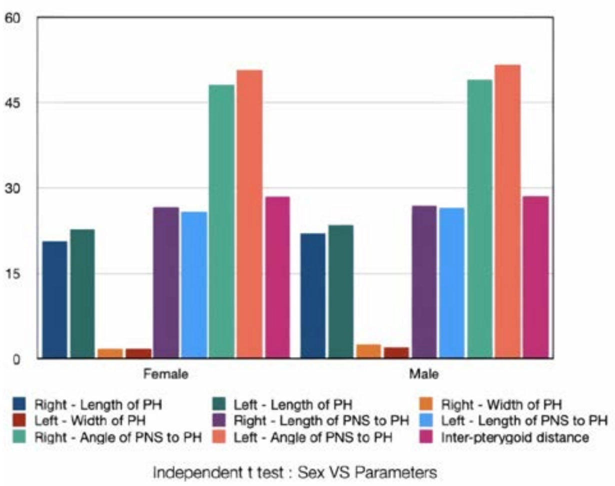

Figure 3: *Independent t test for variance in male and female*

Table 4: Independent Samples T-Test (Sex VS Parameters)

Doppler Indices	t	df	p
Right - Length of PH (in mm)	-1.829	98	0.070
Left - Length of PH (in mm)	-1.130	98	0.261
Right - Width of PH (in mm)	-3.143	98	***0.002***
Left - Width of PH (in mm)	-1.759	98	0.082
Right Length of PNS to PH (in mm)	-0.373	98	0.710
Left Length of PNS to PH (in mm)	-1.117	98	0.267
Right Angle of PNS to PH (in ˚)	-0.995	98	0.322
Left Angle of PNS to PH (in ˚)	-0.927	98	0.356
Inter-pterygoid Distance (in mm)	-0.450	98	0.653

Table 5, showing ANOVA results for age groups versus various parameters, shows significant differences across age groups for all measured parameters. The F-value is 2.968, and the p-value is 0.036. The sum of squares for the right PH length is 114.608. The F-value is 3.687, and the p-value is 0.015.

The sum of squares for the left PH length is 140.104. However, the PH dimensions on both sides, as well as the distances and angles from the PNS to the PH, do not demonstrate any significant differences, with all p-values exceeding 0.05. For example, the p-value of the right PH width is 0.884, whereas the p-value of the left PH width is 0.824.

The inter-pterygoid distance does not exhibit a significant variation, as evidenced by a p-value of. 0.671. (Table 5 and Figure 4)

Table 5: ANOVA- Age Groups VS Parameters

Parameters	**Sum of Squares**	**df**	**Mean Square**	**F**	**p**
Right - Length of PH (in mm)	114.608	3	38.203	2.968	0.036
Left - Length of PH (in mm)	140.104	3	46.701	3.687	***0.015***
Right - Width of PH (in mm)	1.015	3	0.338	0.218	0.884
Left - Width of PH (in mm)	0.767	3	0.256	0.302	0.824
Right Length of PNS to PH (in mm)	9.026	3	3.009	0.291	0.832
Left Length of PNS to PH (in mm)	56.459	3	18.820	1.884	0.137
Right Angle of PNS to PH (in ˚)	93.147	3	31.049	2.149	0.099
Left Angle of PNS to PH (in ˚)	115.692	3	38.564	1.636	0.186
Inter-pterygoid Distance (in mm)	7.748	3	2.583	0.518	0.671

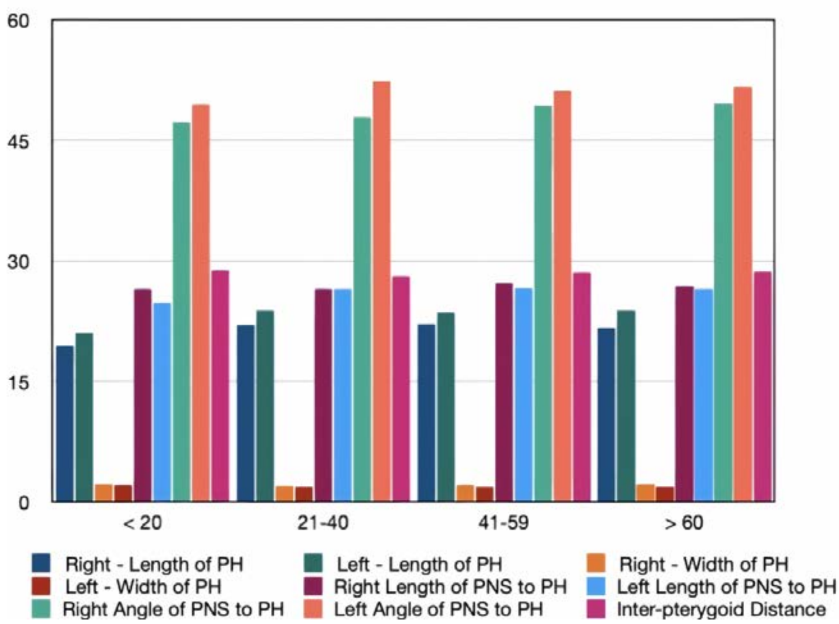

Figure 4: *ANOVA test to compare the parameters across the age group.*

Discussion

The ontogenesis of the pterygoid hamulus, an osseous projection of the medial pterygoid plate, is intrinsically linked to its multifaceted clinical significance. This structure undergoes a complex developmental trajectory, initiating as a cartilaginous precursor in the foetal period and progressively ossifying through childhood and adolescence. The hamulus's morphogenesis is influenced by both genetic factors and biomechanical stresses, particularly those exerted by the tensor veli palatini muscle. This developmental process culminates in the formation of a structure that serves as a critical fulcrum for palatal function and craniofacial biomechanics [6]. The clinical ramifications of hamular development are manifold: aberrations in its morphology or position can precipitate various orofacial pain syndromes, including hamular bursitis and neuralgia [7].

Moreover, the hamulus's role as an attachment point for the pterygomandibular raphe underscores its importance in maintaining proper oral and pharyngeal function [2]. In the realm of orthodontics and orthognathic surgery, a comprehensive understanding of hamular development is paramount for accurate treatment planning and prognostication, particularly in cases involving maxillary expansion or advancement. Furthermore, the hamulus's proximity to critical neurovascular structures necessitates a thorough appreciation of its developmental variations in the context of regional anaesthesia and surgical interventions in the posterior maxillary region. Thus, the developmental trajectory of the pterygoid hamulus is inextricably linked to its diverse clinical implications, emphasising the need for continued research into its morphogenesis across different populations and age groups [8].

Length of Pterygoid Hamulus:

The present study reveals asymmetry in pterygoid hamulus (PH) length between the right and left sides across different age groups. The right PH exhibits greater length in individuals aged 20-59 years, with a slight reduction observed in those over 60. Conversely, the left PH demonstrates minimal length in subjects over 20 years old, reaching its apex in the elderly cohort. Extant literature presents conflicting data regarding age-related PH length alterations. Putz and Kroyer's investigation of a German population suggested PH elongation until maturity, followed by dimensional stability throughout life [9]. In contrast, Krmpotić-Nemanić et al.'s findings in a Croatian population align more closely with our results, indicating a progressive increase in PH length from childhood to adulthood, followed by a significant reduction in elderly subjects [10]. They posit that adult PH elongation may be attributed to buccopharyngeal raphe attachment and masticatory stress. The authors further hypothesise that PH elongation in children ceases upon reaching the buccinator crest, while senescent PH shortening may result from edentulism and a consequent reduction in mechanical stress [10].

Width of the Pterygoid Hamulus:

The width of the pterygoid hamulus is a crucial morphometric parameter in dentistry and maxillofacial surgery, influencing the efficacy of surgical interventions, denture fit, and orthodontic assessments [11]. PH width variations can impact denture comfort, orthodontic treatment planning, and surgical complexity. Notably, increased PH width may predispose to hamular bursitis [12]. This study represents the fourth CBCT-based analysis of PH width, contributing to the limited existing literature. While Orhan et al. reported no significant bilateral differences in PH width, our findings reveal statistically significant asymmetry, with the right PH demonstrating greater width and age-related increases [13]. This contrasts with Romoozi et al.'s observations of bilateral age-related width reduction [14]. The aetiology of increased PH width may be multifactorial, encompassing developmental variations, mechanical stress, prolonged mastication, ossification disparities, pathological processes, and post-traumatic remodelling [15].

Angle formed by the Pterygoid Hamulus to the Posterior Nasal Spine:

This study reveals significant bilateral asymmetry in the angle formed between the pterygoid hamulus (PH) and posterior nasal spine (PNS), with a larger angle observed on the left side (51.59°) compared to the right (48.91°). Gender-based differences were found to be negligible. These findings contrast with Orhan et al.'s study, which reported no significant bilateral differences and smaller angles (left: 33.4°, right: 34.3°) [13]. Unlike Orhan et al.'s observations of symmetrical PNS-

PH distances, our study demonstrates significant bilateral variation, with greater length on the right side. The precise understanding of PH-PNS angular and linear relationships is critical for various surgical procedures, particularly in addressing velopharyngeal insufficiency [16]. For instance, the velo-uvulo-pharyngeal lift procedure, utilised in snoring management, relies on accurate knowledge of these anatomical relationships for successful soft palate manipulation and anchoring [17]. Anatomical variations in these structures may significantly impact surgical outcomes, underscoring the importance of comprehensive preoperative assessment and population-specific morphometric data in maxillofacial and otolaryngological interventions.

Interpterygoid distance:

The inter-pterygoid distance is a critical metric in surgical planning for obstructive sleep apnea syndrome (OSAS), delineating the span between pterygomandibular ligaments and the lateral boundary for pharyngoplasty. Kuzucu et al.'s investigation of 74 OSAS patients revealed mean inter-pterygoid distances of 30.18 ± 1.28, 30.38 ± 2.26, and 28.35 ± 0.82 mm for mild, moderate, and severe OSAS, respectively [18]. Their findings indicated a statistically significant reduction in inter-pterygoid distance in severe OSAS cases compared to mild and moderate presentations. In contrast, our study yielded a mean inter-pterygoid distance of 28.52 ± 2.21 mm, with no significant variations observed between genders or sides. This discrepancy in findings underscores the need for further research to elucidate the relationship between inter-pterygoid distance and OSAS severity across diverse populations, potentially informing more tailored surgical approaches and improving patient outcomes.

Conclusion

In conclusion, this comprehensive morphometric analysis of the pterygoid hamulus (PH) utilising cone beam computed tomography (CBCT) has yielded significant insights into its anatomical variations across different age groups and between bilateral structures. The study reveals noteworthy asymmetries in PH length, width, and angulation relative to the posterior nasal spine, contributing valuable data to the limited existing literature on this clinically significant structure. Our findings underscore the dynamic nature of PH morphology throughout the lifespan, potentially influenced by factors such as masticatory stress, ossification patterns, and age-related changes. The observed variations in PH dimensions and spatial relationships have profound implications for various dental and maxillofacial procedures, including denture fabrication, orthognathic surgery, and the management of orofacial pain syndromes. Furthermore, the study's examination of inter-pterygoid distance provides crucial data for surgical planning in obstructive sleep apnea syndrome (OSAS) interventions. While our results occasionally diverge from previous investigations, these discrepancies highlight the necessity for population-specific morphometric analyses and standardised imaging protocols. The limitations of sample size and specific CBCT parameters in this study emphasise the need for larger-scale, multi-centric investigations to establish more comprehensive normative data. Ultimately, this research contributes to the growing body of knowledge on PH morphometrics, potentially enhancing diagnostic accuracy, treatment planning, and surgical outcomes in various fields of dentistry and maxillofacial surgery. **R**

Author Contributions:

Conceptualization: Eswari Solayappan, Monica Mirnalini M N, Karthikeya Patil

Data curation: Eswari Solayappan, Monica Mirnalini M N

Data Analysis: Varusha Sharon Christopher, Sanjay C J

Writing-original draft: Monica Mirnalini M N

Writing- review and editing: Karthikeya Patil, Sanjay C J, Varusha Sharon Christopher

References

1. Larrabee WF, Makielski KH, Henderson JL. Surgical Anatomy of the Face. Lippincott Williams & Wilkins; 2004. 195 p.
2. Malkidou N, Chaidas K, Thomaidis V, Vassiou K, Fiska A. Pterygoid Hamulus: Morphological Analysis and Clinical Implications. Cureus. 2024 Mar;16(3):e55694.
3. Nimigean V, Nimigean VR, Buţincu L, Sălăvăstru DI, Podoleanu L. Anatomical and clinical considerations regarding the greater palatine foramen. Rom J Morphol Embryol. 2013;54(3 Suppl):779–83.
4. Charbeneau TD, Blanton PL. The pterygoid hamulus. A consideration in the diagnosis of posterior palatal lesions. Oral Surg Oral Med Oral Pathol. 1981 Dec;52(6):574–6.
5. Urban R, Haluzová S, Strunga M, Surovková J, Lifková M, Tomášik J, et al. AI-Assisted CBCT Data Management in Modern Dental Practice: Benefits, Limitations and Innovations. Electronics. 2023 Apr 4;12(7):1710.
6. Kitamura H. Embryology of the Mouth and Related Structures. Maruzen; 1989. 407 p.
7. von Arx T, Lozanoff S. Clinical Oral Anatomy: A Comprehensive Review for Dental Practitioners and Researchers. Springer; 2016. 561 p.
8. Komarnitki I, Mańkowska-Pliszka H, Ungier E, Dziedzic D, Grzegorczyk M, Tomczyk A, et al. Functional morphometry of the pterygoid hamulus. A comparative study of modern and medieval populations. Anthropological Review. 2019 Dec 1;82:389–95.
9. Putz R, Kroyer A. Functional morphology of the pterygoid hamulus. Ann Anat. 1999 Jan;181(1):85–8.
10. Marušić A, Vinter I, Krmpotić-Nemanić J. Lost and found anatomical terms: Crista choanalis vomeris. Annals of Anatomy - Anatomischer Anzeiger. 2006 May 8;188(3):281–3.
11. Annapoorani S, Christy AW, Thambi TJR, Mahalakshmi R. A Preliminary Radiological Study Emphasizing on Anatomic Patterns of Pterygoid Plates Using Cone Beam Computed Tomography. Journal of Indian Academy of Oral Medicine and Radiology. 2023;35(1):87.
12. Thukral H, Nagori SA, Rawat A, Jose A. Pterygoid Hamulus Bursitis: A Rare Intra-Oral Pain Syndrome. J Craniofac Surg. 2019 Oct;30(7):e643–5.
13. Orhan K, Sakul BU, Oz U, Bilecenoglu B. Evaluation of the pterygoid hamulus morphology using cone beam computed tomography. Oral Surg Oral Med Oral Pathol Oral Radiol Endod. 2011 Aug;112(2):e48–55.
14. Romoozi E, Razavi SH, Barouti P, Rahimi M. Investigating the morphologic indices of the hamulus pterygoid process using the CBCT technique. Journal of Research in Medical and Dental Science. 2018;6:240–4.
15. Shetty SS, Shetty P, Shah PK, Nambiar J, Agarwal N. Pterygoid Hamular Bursitis: A Possible Link to Craniofacial Pain. Case Rep Surg. 2018 Aug 12;2018:5108920.
16. Fersing C, Thevarajah D, Sanquer E, Chapuis C, Amelot A, Fougeron C, et al. Validation of an objective assessment tool for velopharyngeal insufficiency in cleft lip and palate children. J Stomatol Oral Maxillofac Surg. 2024 Jul 11;101968.
17. Raol N, Hartnick CJ. Anatomy and physiology of velopharyngeal closure and insufficiency. Adv Otorhinolaryngol. 2015 Feb 19;76:1–6.
18. Kuzucu I, Parlak IS, Baklaci D, Guler I, Kum RO, Ozcan M. Morphometric evaluation of the pterygoid hamulus and upper airway in patients with obstructive sleep apnea syndrome. Surg Radiol Anat. 2020 May;42(5):489–96.

READY - MADE CITATION

Dr. Karthikeya Patil, Dr. Sanjay C J, Dr. Monica Mirnalini M N, Dr. Varusha Sharon Christopher, Dr. Eswari Solayappan. Morphological Characterization of the Pterygoid Hamulus Using Cone Beam Computed Tomography, *Hell J Radiol 2025*; 10(3): 27-36.